

# Interactive Affordance Learning through Manipulation Relationship Graph Construction

Chao Tang<sup>1</sup>, Jingwen Yu<sup>1,2</sup>, Weinan Chen<sup>1</sup>, *Member, IEEE*, and Hong Zhang<sup>1\*</sup> *Fellow, IEEE*

**Abstract**—In this paper, we propose Manipulation Relationship Graph (*MRG*), a novel affordance representation which captures the underlying manipulation relationships of an arbitrary scene. To construct such graph from raw visual observation, a deep neural network named *AffRel* is introduced. It consists of a *Attribute* and *Context* module, which guide the relationship learning at instance and subgraph level respectively. We quantitatively validate our method on a novel manipulation relationship dataset named *SMRD* dataset. To evaluate the performance of proposed model and representation, both visual and physical experiments are conducted. Overall, *AffRel* along with *MRG* outperforms all baselines, achieving the success rate of 88.89% on task relationship recognition (TRR) and 73.33% on task completion (TC). It demonstrates its superior capability to reason about the affordance in an interactive way for the purpose of robotic manipulation.

## I. INTRODUCTION

Recent advances in Artificial Intelligence (AI), Machine Learning (ML) and robotics have inspired the emergence and development of embodied AI [1]. Compared to the so called "internet AI" which focuses on learning from data curated from the internet (e.g. ImageNet [2], COCO [3]) and does not impact our lives physically, embodied AI requires intelligent agents such as robots to perceive and interact with real world entities. In robotics, one way to realize embodied AI is through affordance learning. Affordance, first mentioned in [4], endows robots the ability to identify potential interactions with human or environment and inform the following robotic manipulation. Extensive researches have been conducted on affordance learning.

Most works in computer vision community cast affordance learning as a segmentation problem [5]–[9]. Object parts sharing the same functionality are segmented and grouped at pixel level and assigned with corresponding affordance category label. These methods treat affordance learning as detecting the property of isolated object and do not consider the interactions among objects. For example, the robot is able to predict the affordance of a knife as "cut" (blade) and "grasp" (handle) but has no idea as to "what to cut" or "where to cut". Contrary to segmentation based approaches, symbolic representation firsts converts detected objects into the embedding space and learn a knowledge graph in an interactive way where nodes denote a set of concepts known to the robot (e.g. apple, mug, bowl) and edges denote a set of possible relations such as affordances [10]–[14]. However, to

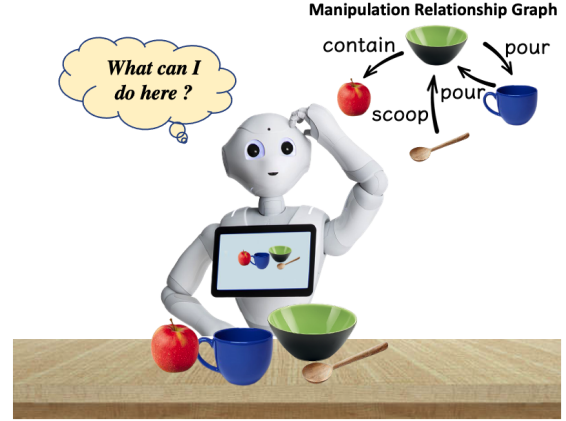


Fig. 1. Robot reasons about the Manipulation Relationship Graph (*MRG*) over a set of kitchen objects.

query the learned knowledge graph, it requires to recognize the object category first using pretrained object detectors such as [15], which holds the closed world assumption and suffer to generalize to novel instances.

To address the problems mentioned above, we introduce Manipulation Relationship Graph (*MRG*), a graph representation which interprets affordance as the interactive manipulation relationships among objects from raw visual observations without category information. As is depicted in Figure 1, the robot first perceives a scene consisting of a set of objects and then abstract it to a Manipulation Relationship Graph, where nodes denote the raw object observations and edges indicate the potential manipulation relationships among objects. Each manipulation relationship is written as a triplet (*subject, relationship, object*), where *subject* and *object* are represented by sequence index (e.g. four objects will give sequence index from 1 to 4). It guides the robotic manipulation by informing "what to use" (*subject*), "how to use" (*relationship*) and "what to act on" (*object*). To construct the *MRG*, we contribute *AffRel*, a novel affordance learning framework which captures the interactive manipulation relationships of an arbitrary scene. It consists of a *Attribute* module and a *Context* module to facilitates model's generalization to in-class, intra-class and inter-class object variations, which will be explained in detail later. For the rest of this paper, we refer to physical entity as **instance** and reserve the term **object** to describe the identity in a relationship triplet (*subject, relationship, object*). Our contributions are three-fold:

- We introduce Manipulation Relationship Graph (*MRG*), a novel affordance representation which captures the underlying manipulation relationship among instances

This work was not supported by any organization

<sup>1</sup>Department of Electronic and Electrical Engineering, Southern University of Science and Technology, China. e-mail: zhangh33@sustech.edu.cn

<sup>2</sup>Department of Computer Science and Engineering, The Hongkong University of Science and Technology, Hongkong, China.

directly from raw visual observation.

- We propose *AffRel*, a neural network structure to infer the manipulation relationships and construct the Manipulation Relationship Graph (*MRG*).
- We contribute a unique dataset, Semantic Manipulation Relationship Dataset (*SMRD*), consisting of 6 manipulation relationship classes, 13 tool categories, 1171 images, 4428 relationship triplets.

The rest of paper is organized as follow. We review related literature in section II and provide the formal definition of *MRG* in section III. The detailed explanation of proposed *AffRel* is given in section IV. Experimental setup and results for both visual and physical experiments are presented in section V and VI respectively. We provide further insights into our work in section VII and conclude the paper in section VIII.

## II. RELATED WORKS

In this paper, we propose to learn affordance in an interactive way by constructing Manipulation Relationship Graph (*MRG*). Therefore, three topics most related are reviewed in this section including affordance learning in robotics, visual relationship detection and manipulation using graph.

### A. Affordance Learning in Robotics

Affordance provides valuable information as to what function the environment affords in pursuit of achieving a specified goal state by robots [4]. There are currently three main types of affordance learning approaches including segmentation based, knowledge-graph based and interaction based, each of which presents a unique way to interpret affordance. For segmentation based method, it segments the object part by functionality at pixel level. [5] starts with segmenting tool affordance regions from local shape and geometry primitives. Built on prior works, [6] utilizes deep learning to achieve state-of-the-art performance on affordance segmentation. While the aforementioned approaches operate on 2D or 2.5D data, [9] segments objects in 3D domain. Segmentation based approaches usually focus on detecting the properties of isolated objects, which does not consider the interactions among instances. Another way to learn affordance is through knowledge graph framework, which captures the relationships among symbols in the embedding space. [10] learns multi-relational embeddings to jointly reason about object affordances, locations, and materials. To keep the knowledge base up-to-date, [13] proposes a incremental robotics knowledge graph framework by leveraging continual learning methods. These method are usually trained on large knowledge sources such as [12] [14]. Knowledge-graph based method models affordance as relationships among instances but it relies on pretrained detector to convert raw visual observations to a set of symbols, which suffers to generalize to novel instances. The third type is to discover affordance through interactions. [16] and [17] learn affordances from goal-directed tool manipulation via a set of predicted keypoints in simulation. Similarly, [18] reasons about the long-term effects of actions

through modeling what actions are afforded in the future through trial-and-error. These models usually dedicate to specific task and are therefore out of our discussion. In contrast to the three categories, the proposed method learns affordance in an interactive manner and is able to understand an arbitrary scene as *MRG* without the need for instance category information, which is particularly helpful in human robot interaction.

### B. Visual Relationship Detection

Visual relationship detection is defined as describing the relationships within the scene from visual input. [19] first proposes to represent instances, attributes and relationships between instances using scene graph. [20] improves on [19] by leveraging languages priors from semantic word embedding to finetune the likelihood of a predicted relationships. After that, numerous methods have been proposed by utilizing recurrent architecture [21], attention mechanism [22] and reinforcement learning [23]. Additionally, visual relationship detection has also been studied in other applications. In object detection, [24] and [25] improve traditional detection pipeline by fusing visual relationship reasoning. [26] focuses on NLP problem and understands referring expression by detecting properties and visual relationships. Also in robotics, [27] detects the support relationships between surface from RGBD data for the purpose of robot navigation while [28] detects the evolution of the spatial relationships between involved instances during manipulation. Our proposed method extends the task of **describing** the scene with spatial or action relationships to **predicting** potential manipulation relationships among instances.

### C. Manipulation Using Graph

Since robotic manipulation necessitates robot executing a sequence of actions in order to achieve a goal, graph becomes a natural spatio-temporal representation. [29] and [30] focus on the problem of robotic grasping. They simultaneously detect instances and recognize the low-level manipulation relationships as a graph to help robots find the right order in which the instances should be grasped. Graph has also been widely used in Task-and-Motion planning (TAMP). [31] solves the long-horizon planning problem by representing subgoals as graphs for rigid-body manipulation and proposes a graph-attention based neural network architecture for processing point cloud inputs. Rather than focusing on symbolic information, [32] jointly predicts a sequence of discrete actions and the parameter values of their associated low-level controllers without prior geometric knowledge of the environment. Combining symbolic and geometric reasoning, [33] builds a two-level scene graph representation including geometric and symbolic scene graph for long-horizon manipulation tasks. Our proposed method focuses on high level scene understanding and uses graph to capture the diverse manipulation relationships among instances.

## III. MANIPULATION RELATIONSHIP GRAPH

Given the observation of a environment scene, our objective is to abstract it to a directed graph, which captures

the underlying manipulation relationships. A set of 6 manipulation relationships are defined: {1-scoop, 2-pour, 3-cut, 4-contain, 5-wipe, 6-dump}. For each scene, let there be  $N$  instances. A manipulation relationship graph  $G = (V, E)$  is constructed, where the vertices  $V = \{v_i\}_{i=1}^N$  represent the raw instance observations in the scene and edges are represented as  $E = \{e_{i,j}\}$  if manipulation relationship exists from instance  $i$  to  $j$  for  $i, j = 1, \dots, N$ . Examples of scene and corresponding manipulation relationship graph are shown in Figure 2.

Each node  $v \in V$  in the graph has a feature vector  $\phi(v)$ , which contains identity, spatial and appearance information. Since category label is not used, instance identity is a 1-dimensional sequence index. Spatial information is represented as 5-dimensional vector indicating the bounding box coordinates and a confidence score. Appearance information is a 512-dimensional feature vector extracted from corresponding spatial location. Edge types and weights (i.e. relationship classes and confidence scores) are inferred using  $\phi(v)$  of all instances.

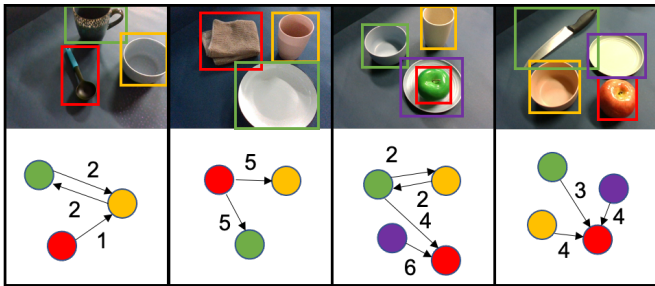


Fig. 2. Examples of scene (first row) and corresponding manipulation relationship graph (second row). Instance indexes are color-coded and manipulation relationships are represented as follow: {1-scoop, 2-pour, 3-cut, 4-contain, 5-wipe, 6-dump}.

#### IV. APPROACH

To address the problem of manipulation relationship graph generation, we present *AffRel*, which takes as input the raw observation of arbitrary scene and outputs the manipulation relationships among instances as *MRG*. An overview of the proposed method is shown in Figure 3. The entire process can be summarized as follow: (1) given the RGB input, category-agnostic instance proposals generated with RPN [15] are grouped into pairs to form a fully-connected graph, where each pair of instances are mutually connected with directed edges; (2) subgraphs are created by taking the union box of two instance proposals; (3) subgraphs referring to the same manipulation relationship are clustered; (4) instance and subgraph features are refined through *Context* and *Attribute* modules; (5) manipulation relationships are predicted based on corresponding subject, object and subgraph features and a *MRG* is then generated. Each step will be explained in detail for the rest of this section.

##### A. FC Graph Construction and Subgraph Clustering

RPN [15] is first adopted to generate the instance proposals. Without prior knowledge, each pair of instances

have possibly mutual manipulation relationships. Therefore, a directed fully-connected graph is constructed as shown in Figure 3 (b), where each instance is connected to all the other instances. Each edge represents the potential manipulation relationship (or no relationship) between subject and object. And each relationship triplet is described as (*subject, relationship, object*).

To obtain the representation for candidate relationship triplet, the union box of subject and object is taken. The corresponding subgraph features are then extracted from the spatial location of union box. Since many subgraphs share the same subject, object and manipulation relationship, subgraph clustering [22] is deployed to merge these subgraphs (shown in Figure 3 (c)). It helps keep the overall graph representation concise and meanwhile save the computation cost. After the clustering, the fully-connected graph consists of two parts: instance proposals and subgraphs. Fully-connected layers and 2-D convolution layers are then applied to instance and subgraph features respectively to obtain the 1-D 512-dimensional instance feature vectors and 2-D  $512 \times 5 \times 5$  subgraph feature maps. Each subgraph is connected to all the instances within it and each candidate relationship triplet refers to one subgraph with corresponding subject and object.

##### B. Attribute Learning as Auxiliary Task

To hold the open-world assumption, the category detection branch is modified to a objectness detection branch. Instead of predicting the category label, it predicts the instance existence label as binary classification ("0" for not instance and "1" for instance), making the proposed method category-agnostic. However, removing the category label leads to a considerable drop in relationship detection performance as category provides important contextual information.

To resolve the dilemma, *Attribute* module is introduced inspired by [8]. The main idea is that the essence of predicting the category label of either subject or object is to recognize its function or attribute and then infer the corresponding manipulation relationship. Meanwhile, attribute is more transferable than category as instances from different categories may share the same attribute. *Attribute* module is added to the detection branch as an auxiliary task. It explicitly predicts the attributes of a given instance (as shown in Figure 4) as a multi-class classification problem with  $R$  outputs, where  $R$  is the amount of manipulation relationship classes (in our case,  $R=6$ ). Based on the fact that visually similar part shares similar functions, *Attribute* module guides instance feature learning by connecting the visual structure to attributes. It helps the proposed method recognize the attributes of novel instances and therefore correctly detect the manipulation relationships. Attribute learning works as a auxiliary task during training and is dropped during inference. Non-affordance instances (e.g. apple) are not considered. The overall detection branch consists of a objectness detection branch, a bounding box regression branch and a attribute prediction branch.

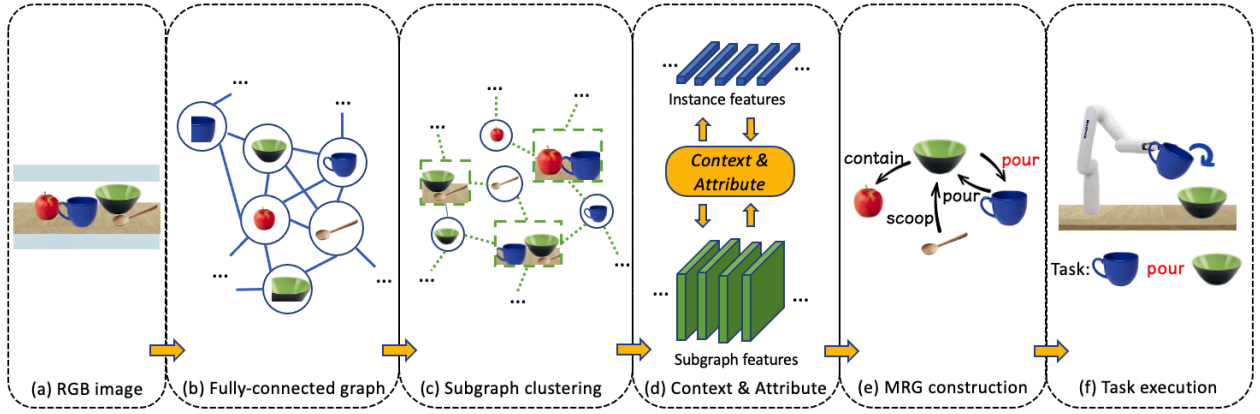


Fig. 3. Overview of the proposed *AffRel*. (a) RGB image capturing a set of instances is used as input. (b) Instance feature proposals (blue) generated by RPN are grouped into pairs to construct a fully-connected graph, where each pair are mutually connected by directed edges. (c) Subgraphs (green) referring to the same manipulation relationship are clustered and merged to keep the graph concise. (d) Instance and subgraph features are refined through *Context* and *Attribute* modules. (e) Manipulation relationships are predicted to build *MRG*. (f) Robot executes the task relationship using computed grasp and effect points.

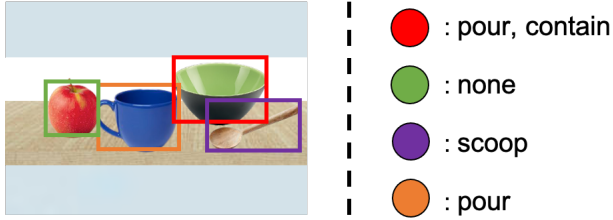


Fig. 4. Attribute prediction as an auxiliary task

### C. Subgraph Feature Aggregation with Context

Instance features offer detailed contextual information such as appearance and spatial location information to facilitate the understanding of how each candidate relationship region interacts with corresponding subject and object. However, raw subgraph feature fails to capture the interactions between itself and instances within it. To resolve this problem, *Context* module modified from [22] is introduced. It is designed based on attention mechanism [34]. The main idea is to aggregate the subgraph feature using the instance features from the corresponding spatial location. The detailed description is as follows. Since different instance locates at different spatial locations within a relationship region, weights should also depend on the locations when incorporating instance features into subgraph features. Let there are  $N$  instances within the subgraph, the weighted instance features at location  $(x, y)$  are expressed below:

$$\hat{\mathbf{O}}(x, y) = \sum_{i=1}^N W(\mathbf{o}_i, S, x, y) \cdot V_{proj}(\mathbf{o}_i) \quad (1)$$

where  $S$  denotes the subgraph feature.  $W(\mathbf{o}_i, S, x, y)$  is attention weight of instance feature  $\mathbf{o}_i$  at  $(x, y)$  and  $\hat{\mathbf{O}}(x, y)$  represents the weighted instance features at the same location.  $V_{proj}$  projects  $\mathbf{o}_i$  to the target subgraph domain. The attention weight is computed as:

$$W(\mathbf{o}_i, S, x, y) = \frac{\exp(K_{proj}(\mathbf{o}_i) \cdot Q_{proj}(S(x, y)))}{\sum_{i=1}^N \exp(K_{proj}(\mathbf{o}_i) \cdot Q_{proj}(S(x, y)))} \quad (2)$$

where  $S(x, y)$  denotes the subgraph feature at  $(x, y)$ .  $K_{proj}$  and  $Q_{proj}$  are projection functions. Then we represent the refined subgraph feature as:

$$\hat{S} = \sum_{x, y} S(x, y) + \alpha \cdot \hat{\mathbf{O}}(x, y) \quad (3)$$

where  $\alpha$  is a learnable scale factor.

### D. Manipulation Relationship Graph Construction

After obtaining the refined instance and subgraph features, manipulation relationship is predicted by taking the addition of corresponding subject, object and subgraph features as follow:

$$p_{i,j} = FC(\text{ReLU}(\mathbf{o}_i + \hat{S} + \mathbf{o}_j)) \quad (4)$$

where  $p_{i,j}$  denotes the relationship (from  $i$  to  $j$ ) distribution over  $R$  types of manipulation relationships plus background (no relationship). Top-1 prediction will be used to form the manipulation relationship triplet as  $(subject, relationship, object)$ , where subject and object are represented by their indexes. Triplet score is computed by taking the product of subject, object and relationship confidence probabilities. Redundant triplets and those with low scores will be eliminated. After that, *MRG* is constructed by treating instances as nodes and relationships among instances as edges with triplet scores being edge weights.

## V. EXPERIMENTAL SETUP

In this section, we first discuss the details of our novel manipulation relationship dataset that is used to evaluate the proposed *AffRel* and other baselines. The setup for both visual and physical experiments are then presented. Finally, the evaluation metrics used for experiments will be given.

### A. SMRD Dataset

In order for robot to learn the interactive affordance and execute various manipulation tasks, a dataset annotated with diverse manipulation relationships is needed. Not aware of



Fig. 5. (a) Experiment platform; (b) Kitchen tools used in SMRD dataset; (c) Intra-class instances; (d) Inter-class instances.

such dataset, Semantic Manipulation Relationship Detection (SMRD) dataset is created. A summary of SMRD dataset is presented in Table I. It includes 13 kitchen tool classes as shown in Figure 5 (b) and 6 relationship classes. Non-affordance instances (e.g. vegetables, fruits) are also collected since manipulation relationships commonly exist between tools with specific affordances and non-affordance instances (e.g. knife cut apple). Overall, SMRD dataset consists of 1171 images and 4428 relationships, averaging 3.78 relationships per image. For each image, the GT relationships are organized in the form of *MRG*. The dataset does not consider the category label since it is not used during relationship inference.

TABLE I  
SUMMARY OF SMRD DATASET

Tool class	pan, spatula, plate, knife, bowl, cloth, fork, mug, spoon, brush, cup, pot, can
Relationship class	scoop, pour, cut, contain, wipe, dump
Image split	988 for training, 183 for testing, 1171 images in total
Relationship split	3563 for training, 865 for testing, 4428 relationships in total

### B. Visual Experiments

To gain deeper insights into our proposed model and show the effectiveness of each component, visual experiments are conducted. We compare *AffRel* to three baselines:

- **Base** uses raw instance and subgraph features. It does not consider the attribute of each instance and isolate the contextual connection between relationship region and instances within it.
- **Base+ATT** refines instance features with *Attribute* module. It guides the relationship learning by explicitly predicting the commonsense attributes of instances. It helps model gain better generalization capability to unseen instances and relationships compared to directly predicting the category label.
- **Base+CT** is equipped with *Context* module. It aggregates subgraph features with instance features from

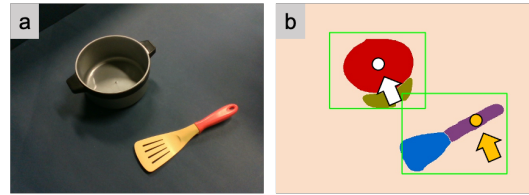


Fig. 6. Grasp point (yellow) and effect point (white) computed using AffordanceNet [6]

corresponding spatial location and therefore guide the model to "look at" the positions where subject and object locate.

- **Base+ATT+CT (proposed)** takes advantage of both *Attribute* and *Context* module. It incorporates attribute learning and context information to obtain better transferability and prediction accuracy.

### C. Physical Experiments

We then evaluate the feasibility of proposed method in robotic manipulation experiments. Figure 5 (a) shows the experiment platform. It consists of a 6-DOF Kinova Gen3 Lite robotic arm and a Intel Realsense D435i RGBD camera with eye-to-hand calibration. In addition to *AffRel*, two types of affordance detection approaches are presented for comparison:

- **AffSeg** represents segmentation-based affordance detection methods [5]–[9]. In these approaches, instance parts sharing the same functionality are segmented and grouped at pixel level, then assigned with corresponding affordance label. In the following comparison, we select state-of-the-art affordance detection architecture [6] for comparison.
- **Det+KG** first detects the instance categories in the given scene and then query the trained knowledge base to infer the manipulation relationships. [11] is reproduced as a baseline approach. It consists of a detector pretrained on SMRD dataset in conjunction with a knowledge graph constructed from GT manipulation relationships for fair comparison.

Since each method above deals with a unique set of affordances, four shared affordances including scoop, pour, cut, contain are extracted for testing. Besides, for the purpose of robotic manipulation, grasp point on subject and effect point on object is computed using AffordanceNet [6]. It is done by first perform affordance segmentation on subject and object. Grasp and effect points are then computed by taking the midpoint of selected affordance regions. As is shown in Figure 6, AffordanceNet segments the pot to a "contain" region (red) and a "w-grasp" region (brown). Spatula is segmented into a "scoop" region (blue) as a "grasp" region (purple). Grasp point (yellow) is the midpoint of "grasp" region on spatula (subject) while effect point (white) is the midpoint of "contain" region on pot (object). Finally, manipulation action is executed using motion primitive.

### D. Evaluation Metric

Two sets of evaluation metrics are provided for visual and physical experiments respectively. For visual experiments,

**Recall@1** (denoted as **R@1**) and **Recall@5** (denoted as **R@5**) are used. We evaluate the performance under the tasks of phrase detection (denoted as **P**) and relationship detection (denoted as **R**). The former task coarsely localizes the entire relationship as one union bounding box having at least 0.5 overlap ground truth box and the latter requires localization of both subject and object with their ground truth boxes and predicts the correct relationship simultaneously. More details can be found in [20]. In all, four metrics including **PR@1**, **PR@5**, **RR@1**, **RR@5** are used in visual experiments. For physical experiments, robot needs to localize each instance precisely for the purpose of manipulation, therefore **RR@1** and **RR@3** are used. To test the task execution capability, task relationship recognition rate (denoted as **TRR**) and task completion rate (denoted as **TC**) are recorded. **TRR** examines robot’s recognition ability towards given task relationship and **TC** evaluates task completion ability.

## VI. EXPERIMENTS

This section details the experiments performed and their outcomes. We first show the results from visual experiments by comparing the proposed methods to three baselines. Three sets of physical experiments are then analyzed to examine the in-class, intra-class and inter-class generalization capabilities.

### A. Visual experiments results

TABLE II  
PERFORMANCE ON VISUAL EXPERIMENTS (%)

Approach	PR@1	PR@5	RR@1	RR@5
Base	28.704	74.884	17.130	59.375
Base+ATT	35.764	82.060	19.792	67.593
Base+CT	35.995	81.597	19.907	67.246
<b>Base+ATT+CT (proposed)</b>	<b>37.384</b>	<b>84.259</b>	<b>20.370</b>	<b>68.059</b>

Visual experiments are performed on SMRD dataset. Four models follow the same training and inference strategies. During training, VGG16 [35] pretrained on ImageNet [2] is used as backbone and Adam [36] is used as optimizer with 0.9 momentum and 0.00001 weight decay. Initial learning rate is set as 0.001 and get multiplied by 0.1 every 5 epochs. Subgraph clustering threshold is set to 0.5. RPN is trained first and then the whole model is trained jointly for 15 epochs. The model is designed based on [15] [22]. During testing phase, triplet NMS [37] is performed to remove redundant predictions if two relationships refer to the same region.

As shown in Table II, the proposed **Base+ATT+CT** outperforms all three baselines across all four metrics. This highlights the model’s ability to accurately recognize manipulation relationships using attribute and context information. **Base** shows the lowest recall since it does not utilize instance attribute information and isolate the connection between relationship region and instances within it. **Base+ATT** gains a performance boost compared to **Base**. It shows the effectiveness of proposed **Attribute** module. Instead of predicting

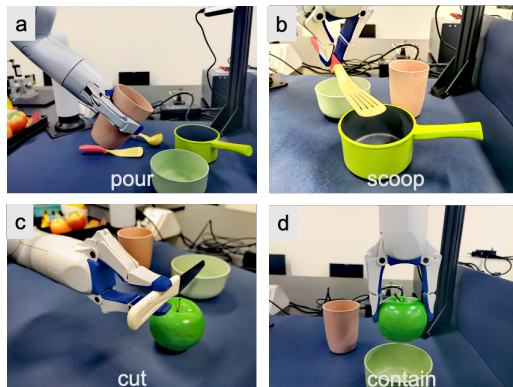


Fig. 7. Examples of manipulation relationships executed by the robot

the category label, it guides the local feature learning by inferring what attributes an instance possess. Attribute is highly transferable across instance categories, which leads to better generalization capability. **Base+CT** also shows competitive performance as it bridges the gap between relationship region and instances within it. Raw subgraph feature fails to capture the spatial and appearance information of subject and object within the region. With **Context**, the model learns both "where to look at" (spatial info) and "what to look at" (appearance info).

### B. MRG guided task execution

For the following three physical tasks, we examine each method’s ability to recall the manipulation relationships and manipulate instances with motion primitive accordingly. Shown in Figure 7 are examples of manipulation relationships executed by the robot. In-class situation is first tested.

TABLE III  
IN-CLASS TASK EXECUTION (%)

Approach	RR@1	RR@3	TRR	TC
AffSeg	23.73	45.41	33.33	33.33
Det+KG	<b>29.29</b>	78.41	86.67	66.67
<b>AffRel (Ours)</b>	29.26	<b>80.64</b>	<b>93.33</b>	<b>80.00</b>

In this task, a set of instances covering all four manipulation relationships (i.e. scoop, pour, cut, contain) are selected from SMRD dataset and construct 15 scenes. Each scene consists of 3-7 relationships and one task relationship is randomly selected from GT relationships. Robot is required to (1) recall the manipulation relationships within the given scene (**RR@k**), (2) recognize the selected task relationship (**TRR**), (3) physically execute the task with motion primitives (**TC**). Results are presented in Table III. **AffSeg** performs the worst. It is because segmentation-based approaches only deal with instances with specific affordances such as tools whereas most manipulation actions happen between tools and non-affordance instances. For example, **AffSeg** fails to recognize and execute the task (*knife, cut, apple*) since apple has no affordance. Therefore, it fails in all "cut" and "contain" tasks. **Det+KG** gives competitive result, leading in **RR@1**. The model is able to output robust detection results and query the knowledge base accordingly

with a few misclassifications. And the misclassifications lead to inferior performance to the proposed method across three metrics as *AffRel* does not rely on instance category to make predictions.

### C. Intra-class generalization

TABLE IV  
INTRA-CLASS GENERALIZATION (%)

Approach	RR@1	RR@3	TRR	TC
AffSeg	18.50	44.17	26.67	26.67
Det+KG	<b>26.83</b>	68.33	86.67	73.33
<i>AffRel (Ours)</i>	26.28	<b>72.72</b>	<b>93.33</b>	<b>80.00</b>

In this task, we investigate whether each model can generalize learned relationships to unseen instances from the same class. As shown in Figure 5 (c), a set of instances sharing the same category with SMRD dataset is collected but varies in color, material and size. 15 scenes are then generated and each scene contains 3-8 manipulation relationships. Table IV details the results. Similarly, *AffSeg* gives the lowest recall and task completion rate. *Det+KG* serves as a strong baseline and performs slightly better than *AffRel* in terms of **RR@1**. A drop occurs on **RR@3** for both *Det+KG* and *AffRel*, showing the large the intra-class variation. The proposed method achieves superior **RR@3**, **TRR** and **TC** due to the category-agnostic design, leading to better task execution ability.

### D. Inter-class generalization

TABLE V  
INTER-CLASS GENERALIZATION (%)

Approach	RR@1	RR@3	TRR	TC
AffSeg	8.73	13.02	20.00	20.00
Det+KG	27.06	51.35	66.67	46.67
<i>AffRel (Ours)</i>	<b>28.17</b>	<b>62.30</b>	<b>80.00</b>	<b>60.00</b>

Figure 5 (d) shows the instances used for inter-class generalization experiment, which is the most challenging task out of three. These instances differs largely from SMRD dataset in usage, appearance and material. Results is shown in Table V. The proposed method outperforms all other baselines across all four metrics by statistically significant margins. Large inter-class variation causes considerable misclassifications to *Det+KG* and therefore leads to inferior performance. *AffSeg* performs the worst as the model does not generalize well to inter-class instances and meanwhile is not able to recognize non-affordance instances.

## VII. DISCUSSION

An overall evaluation of three methods is presented in Figure 8 by combining the statistics from three sets of physical experiments. The proposed method shows clear superiority under each evaluation metric. Besides, a significant drop from **TRR** to **TC** is observed, showing the gap between relationship recognition and successful manipulation. It is

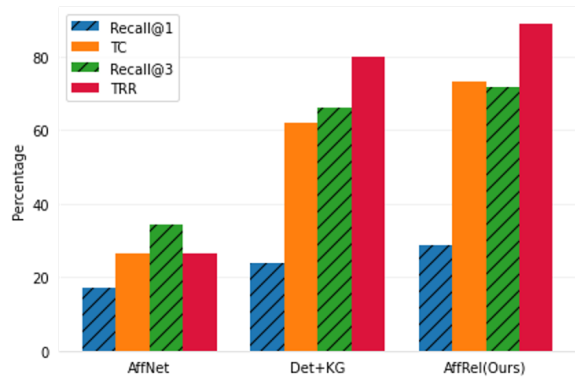


Fig. 8. Overall performance (%) of three methods in physical experiments

mainly caused by two reasons. First, manipulation action is implemented as pre-designed motion primitives, which does not consider the task and environment constraints. Low-level task and motion planning (TAMP) algorithm can be combined to generate flexible manipulation primitives. Another typical failure case is due to sub-optimal grasp point. As is shown in Figure 9, grasp point computed using [6] drifts away from the GT grasp point annotated by human, which leads to unstable grasping and potential manipulation failure. It indicates that task-oriented grasping (TOG) module [16] [38] is needed to further improve the task execution capability.

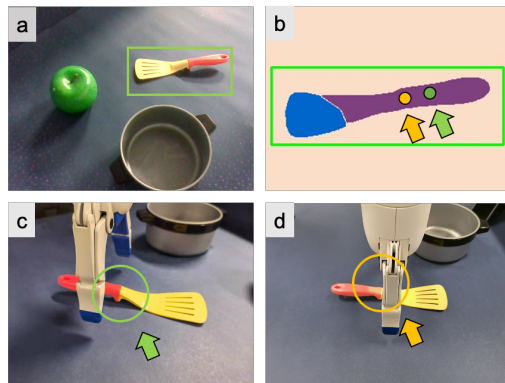


Fig. 9. Human annotated (GT) grasp point (green) and computed grasp point (yellow)

## VIII. CONCLUSIONS

This work addresses the problem of affordance learning in the task of robotic manipulation. We introduce a novel affordance representation which captures the potential manipulation relationships of a arbitrary scene. A deep neural network is designed to construct the proposed Manipulation Relationship Graph from raw visual observation. To train the model, a novel manipulation relationship dataset is collected and annotated, consisting of 6 manipulation relationship classes and 13 tool categories. Visual and physical experiments demonstrate the superiority of proposed model and representation against all baselines.

## ACKNOWLEDGMENT

The preferred spelling of the word "acknowledgment" in America is without an "e" after the "g". Avoid the stilted expression, "One of us (R. B. G.) thanks . . ." Instead, try

ÖR. B. G. thanks Ó. Put sponsor acknowledgments in the unnumbered footnote on the first page.

#### REFERENCES

- [1] R. Pfeifer and F. Iida, "Embodied artificial intelligence: Trends and challenges," in *Embodied artificial intelligence*. Springer, 2004, pp. 1–26.
- [2] A. Krizhevsky, I. Sutskever, and G. E. Hinton, "Imagenet classification with deep convolutional neural networks," *Advances in neural information processing systems*, vol. 25, pp. 1097–1105, 2012.
- [3] T.-Y. Lin, M. Maire, S. Belongie, J. Hays, P. Perona, D. Ramanan, P. Dollár, and C. L. Zitnick, "Microsoft coco: Common objects in context," in *European conference on computer vision*. Springer, 2014, pp. 740–755.
- [4] J. J. Gibson, "The theory of affordances," *Hilldale, USA*, vol. 1, no. 2, pp. 67–82, 1977.
- [5] A. Myers, C. L. Teo, C. Fermüller, and Y. Aloimonos, "Affordance detection of tool parts from geometric features," in *2015 IEEE International Conference on Robotics and Automation (ICRA)*. IEEE, 2015, pp. 1374–1381.
- [6] T.-T. Do, A. Nguyen, and I. Reid, "Affordancenet: An end-to-end deep learning approach for object affordance detection," in *2018 IEEE international conference on robotics and automation (ICRA)*. IEEE, 2018, pp. 5882–5889.
- [7] R. Xu, F.-J. Chu, C. Tang, W. Liu, and P. A. Vela, "An affordance keypoint detection network for robot manipulation," *IEEE Robotics and Automation Letters*, vol. 6, no. 2, pp. 2870–2877, 2021.
- [8] F.-J. Chu, R. Xu, C. Tang, and P. A. Vela, "Recognizing object affordances to support scene reasoning for manipulation tasks," *arXiv preprint arXiv:1909.05770*, 2019.
- [9] S. Deng, X. Xu, C. Wu, K. Chen, and K. Jia, "3d affordancenet: A benchmark for visual object affordance understanding," in *Proceedings of the IEEE/CVF Conference on Computer Vision and Pattern Recognition*, 2021, pp. 1778–1787.
- [10] A. Daruna, W. Liu, Z. Kira, and S. Chetnova, "Robocse: Robot common sense embedding," in *2019 International Conference on Robotics and Automation (ICRA)*. IEEE, 2019, pp. 9777–9783.
- [11] A. Saxena, A. Jain, O. Sener, A. Jami, D. K. Misra, and H. S. Koppula, "Robobrain: Large-scale knowledge engine for robots," *arXiv preprint arXiv:1412.0691*, 2014.
- [12] M. Beetz, D. Beßler, A. Haidu, M. Pomarlan, A. K. Bozcuoğlu, and G. Bartels, "Know rob 2.0—a 2nd generation knowledge processing framework for cognition-enabled robotic agents," in *2018 IEEE International Conference on Robotics and Automation (ICRA)*. IEEE, 2018, pp. 512–519.
- [13] A. Daruna, M. Gupta, M. Sridharan, and S. Chernova, "Continual learning of knowledge graph embeddings," *IEEE Robotics and Automation Letters*, vol. 6, no. 2, pp. 1128–1135, 2021.
- [14] H. Liu and P. Singh, "Conceptnet—a practical commonsense reasoning tool-kit," *BT technology journal*, vol. 22, no. 4, pp. 211–226, 2004.
- [15] S. Ren, K. He, R. Girshick, and J. Sun, "Faster r-cnn: Towards real-time object detection with region proposal networks," *Advances in neural information processing systems*, vol. 28, pp. 91–99, 2015.
- [16] Z. Qin, K. Fang, Y. Zhu, L. Fei-Fei, and S. Savarese, "Keto: Learning keypoint representations for tool manipulation," in *2020 IEEE International Conference on Robotics and Automation (ICRA)*. IEEE, 2020, pp. 7278–7285.
- [17] D. Turpin, L. Wang, S. Tsogkas, S. Dickinson, and A. Garg, "Gift: Generalizable interaction-aware functional tool affordances without labels," *arXiv preprint arXiv:2106.14973*, 2021.
- [18] D. Xu, A. Mandlekar, R. Martín-Martín, Y. Zhu, S. Savarese, and L. Fei-Fei, "Deep affordance foresight: Planning through what can be done in the future," *arXiv preprint arXiv:2011.08424*, 2020.
- [19] J. Johnson, R. Krishna, M. Stark, L.-J. Li, D. Shamma, M. Bernstein, and L. Fei-Fei, "Image retrieval using scene graphs," in *Proceedings of the IEEE conference on computer vision and pattern recognition*, 2015, pp. 3668–3678.
- [20] C. Lu, R. Krishna, M. Bernstein, and L. Fei-Fei, "Visual relationship detection with language priors," in *European conference on computer vision*. Springer, 2016, pp. 852–869.
- [21] D. Xu, Y. Zhu, C. B. Choy, and L. Fei-Fei, "Scene graph generation by iterative message passing," in *Proceedings of the IEEE conference on computer vision and pattern recognition*, 2017, pp. 5410–5419.
- [22] Y. Li, W. Ouyang, B. Zhou, J. Shi, C. Zhang, and X. Wang, "Factorizable net: an efficient subgraph-based framework for scene graph generation," in *Proceedings of the European Conference on Computer Vision (ECCV)*, 2018, pp. 335–351.
- [23] X. Liang, L. Lee, and E. P. Xing, "Deep variation-structured reinforcement learning for visual relationship and attribute detection," in *Proceedings of the IEEE conference on computer vision and pattern recognition*, 2017, pp. 848–857.
- [24] Y. Liu, R. Wang, S. Shan, and X. Chen, "Structure inference net: Object detection using scene-level context and instance-level relationships," in *Proceedings of the IEEE conference on computer vision and pattern recognition*, 2018, pp. 6985–6994.
- [25] J. Sawatzky, Y. Souri, C. Grund, and J. Gall, "What object should i use?-task driven object detection," in *Proceedings of the IEEE/CVF Conference on Computer Vision and Pattern Recognition*, 2019, pp. 7605–7614.
- [26] V. K. Nagaraja, V. I. Morariu, and L. S. Davis, "Modeling context between objects for referring expression understanding," in *European Conference on Computer Vision*. Springer, 2016, pp. 792–807.
- [27] M. Y. Yang, W. Liao, H. Ackermann, and B. Rosenhahn, "On support relations and semantic scene graphs," *ISPRS journal of photogrammetry and remote sensing*, vol. 131, pp. 15–25, 2017.
- [28] K. Zampogiannis, Y. Yang, C. Fermüller, and Y. Aloimonos, "Learning the spatial semantics of manipulation actions through preposition grounding," in *2015 IEEE international conference on robotics and automation (ICRA)*. IEEE, 2015, pp. 1389–1396.
- [29] H. Zhang, X. Lan, X. Zhou, Z. Tian, Y. Zhang, and N. Zheng, "Visual manipulation relationship network for autonomous robotics," in *2018 IEEE-RAS 18th International Conference on Humanoid Robots (Humanoids)*. IEEE, 2018, pp. 118–125.
- [30] D. Park, Y. Seo, D. Shin, J. Choi, and S. Y. Chun, "A single multi-task deep neural network with post-processing for object detection with reasoning and robotic grasp detection," in *2020 IEEE International Conference on Robotics and Automation (ICRA)*. IEEE, 2020, pp. 7300–7306.
- [31] A. Simeonov, Y. Du, B. Kim, F. R. Hogan, J. Tenenbaum, P. Agrawal, and A. Rodriguez, "A long horizon planning framework for manipulating rigid pointcloud objects," *arXiv preprint arXiv:2011.08177*, 2020.
- [32] D. Driess, J.-S. Ha, R. Tedrake, and M. Toussaint, "Learning geometric reasoning and control for long-horizon tasks from visual input," in *Proc. of the IEEE International Conference on Robotics and Automation (ICRA)*, 2021.
- [33] Y. Zhu, J. Tremblay, S. Birchfield, and Y. Zhu, "Hierarchical planning for long-horizon manipulation with geometric and symbolic scene graphs," *arXiv preprint arXiv:2012.07277*, 2020.
- [34] A. Vaswani, N. Shazeer, N. Parmar, J. Uszkoreit, L. Jones, A. N. Gomez, Ł. Kaiser, and I. Polosukhin, "Attention is all you need," in *Advances in neural information processing systems*, 2017, pp. 5998–6008.
- [35] K. Simonyan and A. Zisserman, "Very deep convolutional networks for large-scale image recognition," *arXiv preprint arXiv:1409.1556*, 2014.
- [36] D. P. Kingma and J. Ba, "Adam: A method for stochastic optimization," *arXiv preprint arXiv:1412.6980*, 2014.
- [37] Y. Li, W. Ouyang, X. Wang, and X. Tang, "Vip-cnn: Visual phrase guided convolutional neural network," in *Proceedings of the IEEE conference on computer vision and pattern recognition*, 2017, pp. 1347–1356.
- [38] W. Liu, A. Daruna, and S. Chernova, "Cage: Context-aware grasping engine," in *2020 IEEE International Conference on Robotics and Automation (ICRA)*. IEEE, 2020, pp. 2550–2556.